TCP Transl Clin Pharmacol
2016;24(1):55-62
http://dx.doi.org/10.12793/tcp.2016.24.1.55

Mixed–effects analysis of increased rosuvastatin absorption by coadministered telmisartan

Wan-Su Park, Dooyeon Jang, Seunghoon Han and Dong-SeokYim*

Department of Clinical Pharmacology and Therapeutics, Seoul St. Mary's Hospital, PIPET (Pharmacometrics Institute for Practical Education and Training), College of Medicine, The Catholic University of Korea, Seoul 06591, Korea

*Correspondence: D. S. Yim; Tel: +82-2-2258-7327, Fax: +82-2-2258-7876, E-mail: yimds@catholic.ac.kr

Received 16 Fed 2015
Revised 24 Fed 2016
Accepted 24 Fed 2016

Keywords
Rosuvastatin,
Telmisartan,
drug-drug interaction,
NONMEM

pISSN: 2289-0882
eISSN: 2383-5427

The C_{max} and AUC of rosuvastatin increase when it is coadministered with telmisartan. The aim of this study was to explore which of the pharmacokinetic (PK) parameters of rosuvastatin are changed by telmisartan to cause such an interaction. We used data from drug–drug interaction (DDI) studies of 74 healthy volunteers performed in three different institutions. Rosuvastatin population PK models with or without telmisartan were developed using NONMEM (version 7.3). The plasma concentration–time profile of rosuvastatin was best described by a two-compartment, first-order elimination model with simultaneous Erlang and zero-order absorption when given rosuvastatin alone. When telmisartan was coadministered, the zero-order absorption fraction of rosuvastatin had to be omitted from the model because the absorption was dramatically accelerated. Notwithstanding the accelerated absorption, the relative bioavailability (BA) parameter estimate in the model demonstrated that the telmisartan-induced increase in BA was only about 20% and the clearance was not influenced by telmisartan at all in the final PK model. Thus, our model implies that telmisartan may influence the absorption process of rosuvastatin rather than its metabolic elimination. This may be used as a clue for further physiologically based PK (PBPK) approaches to investigate the mechanism of rosuvastatin–telmisartan DDI.

ORIGINAL ARTICLE

Introduction

The 3-hydroxy-3-methylglutaryl coenzyme A reductase inhibitor rosuvastatin (Crestor) effectively reduces low-density lipoprotein cholesterol levels in dyslipidemic patients.[1] Following intravenous administration of rosuvastatin, clearance is predominantly nonrenal, with hepatic and renal routes of elimination accounting for 72% and 28% of total systemic clearance, respectively.[2] Rosuvastatin is mainly excreted unchanged into bile,[2,3] and less than 10% is metabolized to *N*-desmethyl rosuvastatin by CYP2C9.[4] Rosuvastatin is extensively distributed into the liver, presumably because of active uptake by organic-anion transporting polypeptides (OATPs)1B1, OATP1B3, and OATP2B1, and by the sodium-dependent taurocholated cotransporting polypeptide (NTCP) transporters,[5–7] despite its low passive diffusion into hepatocytes.[3,8,9] It is also a substrate of efflux transporters such as the liver canalicular and intestinal breast cancer resistance protein (BCRP).[10]

Among patients with cardiovascular disease in a three-year retrospective study, 30.7% were found to have both hypertension and dyslipidemia, and 66.3% of patients with diabetes had concomitant hypertension and dyslipidemia.[11] Thus, multiple drug therapy has been widely practiced to treat problems including hypertension and dyslipidemia. Rosuvastatin is commonly used in combination with telmisartan, an angiotensin II type-I receptor antagonist (ARB). Recently, Son et al.[12] reported increased pharmacokinetic (PK) exposure of rosuvastatin when coadministered with telmisartan. The absorption of rosuvastatin was accelerated (C_{max} was doubled, with T_{max} change from 5 h to 0.75 h), whereas its AUC increased by only 1.18-fold when coadministered with telmisartan, although the cause of this phenomenon was not identified by the authors. In Korea, several PK studies of rosuvastatin and telmisartan interaction with similar designs have been conducted that showed the same trend of increased exposure of rosuvastatin. However, one peculiar finding in the studies performed at different institutions was that the level of rosuvastatin PK exposure was significantly different by the contact research organizations (CROs)

that measured the rosuvastatin plasma concentrations.

The aim of this study was to use mixed effect modeling to explore which of the PK parameters of rosuvastatin are changed by telmisartan. Although the interinstitutional differences discussed in this report may be a sensitive issue for the CROs or regulatory authority, they should not be overlooked, because the reliability and comparability of concentration measurement data is one of fundamentals in research and development. Thus, we did not reveal the identity of institutions, sponsors, or CROs that were involved in the production of the PK data after discussion with the editors of Translational and Clinical Pharmacology.

Methods

Study design and data

The rosuvastatin pharmacokinetics data following oral administration of rosuvastatin alone or rosuvastatin with coadministration of telmisartan to healthy volunteers were available from three different clinical trial centers. These data came from 74 participants enrolled in three clinical drug interaction studies to evaluate the effect of telmisartan on the PK of rosuvastatin. Studies conducted in institutions A (Inst_A) and C (Inst_C) employed a one-sequence crossover design, while that in institution B (Inst_B) employed a two-way crossover design.

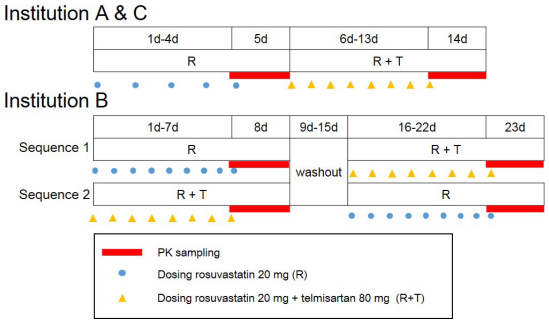

Figure 1. Overall study schedules and dosage regimens.

All participants were randomly allocated to the two treatment groups (rosuvastatin with/without telmisartan) and received multiple doses of 20 mg rosuvastatin or 80 mg telmisartan to reach a steady state. PK sampling schemes, dosage regimen, and study designs in the three different institutions are illustrated in Figure 1. The detailed sampling time points, number of participants, number of samples used for data analysis and demographic characteristics of the volunteers at each institution are summarized in Table 1.

Each study protocol was approved by the ethics committees at participating study centers and all studies were conducted in accordance with the principles of the Declaration of Helsinki and Korean good clinical practice. Samples were analyzed using a high-performance liquid chromatography mass spectrometry method (HPLC-MS/MS) at different CROs. The range of the lower limits of quantitation were 0.1–1 ng/mL.

Noncompartmental Analysis

Noncompartmental analysis (NCA, Phoenix WinNonlin, version 6.3, Pharsight Corporation, CA, USA) was performed to determine the PK parameters of rosuvastatin. PK parameters including terminal half-life ($t_{1/2}$), area under the concentration–time curve over the dosing interval at steady state ($AUC_{\tau,ss}$), maximum concentration at steady state ($C_{max,ss}$) and time at which occurs $C_{max,ss}$ ($T_{max,ss}$) were calculated. $AUC_{\tau,ss}$ was calculated using a linear trapezoidal with linear interpolation method and $t_{1/2}$ was calculated as $0.693/\lambda_z$, where λ_z is the terminal elimination rate constant. $C_{max,ss}$ and $T_{max,ss}$ were determined directly from the observed data. All analyses were made using the actual sampling times rather than the scheduled times.

Population PK Model Development

The population PK modeling was conducted using NONMEM (version 7.3, Icon Development Solutions, Ellicott City, MD, USA) with Pirana (version 2.9.2). RStudio (version 0.99) using R (version 3.2.2) and Xpose4 (version 4.5.3) were used for data preparation, graphical analysis, model diagnostics, and statistical summaries. A first-order conditional estimation method with interaction (FOCEI) was used for parameter estimation.

Table 1. Summary of demographics and sampling schemes

Institution	Subjects	Samples	Sampling points (h)	Age (years)	Height (cm)	Weight (kg)
A	31	754	Predose, 0.5, 1, 2, 3, 4, 5, 6, 8, 10, 12, 16, 24	24.1 (20-33)	175 (161.0-183.0)	69.8 (59.1-85.6)
B	20	570	Predose, 0.33, 0.66, 1, 1.5, 2, 3, 4, 5, 6, 7, 8, 10, 12, 24	24.7 (19-33)	176.6 (167.2-187.3)	70.1 (60.0-84.0)
C	23	598	Predose, 0.33, 0.66, 1, 2, 3, 4, 5, 6, 8, 10, 12, 24	23.7 (19-34)	171.3 (160.3-182.4)	67.2 (54.2-79.0)
Total	74	1922	-	24.2 (19-34)	174.3 (160.3-187.3)	69.1 (54.2-85.6)

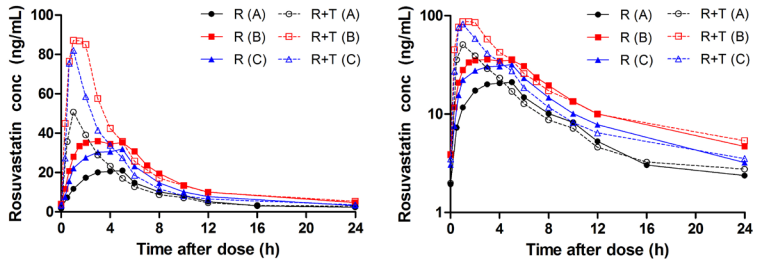

Figure 2. Mean plasma concentration-time profiles of rosuvastatin following oral administration of rosuvastatin 20 mg alone (R) or rosuvastatin 20 mg with telmisartan 80 mg (R+T) per institution (A, B, C). Linear and semilogarithmic scales shown on left and right panels, respectively.

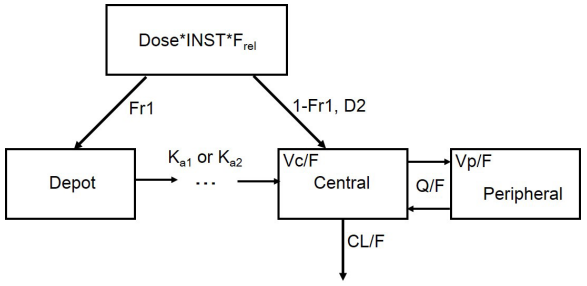

Figure 3. Rosuvastatin PK models. INST, institutional difference (fixed as 1 for institutiona A); F_{rel}, relative bioavailability of rosuvastatin with telmisartan (fixed as 1 for without telmisartan group); Fr1, fraction of the dose absorbed through the Erlang absorption (fixed as 1 for with telmisartan group); D2, duration of zero-order absorption (fixed as 0 for with telmisartan); K_{a1}, absorption rate constant without telmisartan; K_{a2}, absorption rate constant with telmisartan; CL/F, apparent clearance; Vc/F, apparent volume of central compartment; Q/F, apparent intercompartmental clearance; Vp/F, apparent volume of peripheral compartment.

Appropriate model structures for rosuvastatin were guided by previous report[13] and the objective function value (OFV), goodness-of-fit plots, precision in parameter estimates, and model stability (i.e., condition number, successful convergence, and matrix singularity). The results for likelihood ratio tests (LRT) were considered to be significant if decreases in the OFV were greater than the cut-off points equivalent to the *p* value 0.05 (i.e., 3.84 for *df* = 1; 5.99 for *df* = 2, etc.). Reported population PK model for rosuvastatin was a two-compartment, with a simultaneous first- and zero-order absorption model. Thus, a two-compartment model with first-order absorption was used as an initial model, and then various absorption models were evaluated. Interindividual variability (IIV) was described using a log-normal distribution of structural model parameters:

$$P_i = P_{TV} \cdot \exp(\eta_i)$$

where P_i is the individual value of the parameter (e.g., CL/F or V_c/F) for individual *i*, P_{TV} is the typical value model parameter, and η_i is the inter-individual random effect accounting for the *i*th individual's deviation from the typical value. The η_i was assumed to have a normal distribution with a mean of zero and variance of ω^2. When the correlation between the random variables was significant, the relationship was reflected in the model using the OMEGA BLOCK option. The coefficient of variation (%CV) is reported as:

$$\%CV\ (IIV) = \sqrt{e^{\omega^2}-1} \cdot 100$$

The residual error model was tested using proportional and combined error models:

$$Y_{ij} = C_{ij} + w_{ij} \cdot \varepsilon_{ij}$$

$$w_{ij} = \sqrt{C_{ij}^2 \sigma_1^2 + \sigma_2^2}$$

where Y_{ij} denotes the observed concentration for the *i*th individual at time t_j; C_{ij} denotes the corresponding predicted concentration based on the PK model, ε_{ij} denotes the intra-individual (residual) random effect (zero mean and unit variance), and w_{ij} denotes the residual standard deviation (SD) with corresponding proportional and additive variance components, σ_1^2 and σ_2^2, respectively.

Model evaluation

The stability of the final model was evaluated by non-parametric bootstrap analysis using Wings for NONMEM (version 741, wfn.sourceforge.net/). The median values and 95% confidence intervals for the parameter estimates from 200 bootstrap replicates of the original dataset were compared with the final parameters. Visual predictive checks (VPC) were performed by using simulated concentrations of 1000 virtual datasets simulated using the final model. The median, 5th, and 95th percentiles of the simulated concentrations were calculated at each time point and were overlaid on the observed concentrations grouped by the institutions and telmisartan coadministration.

Results

Noncompartmental analysis

The mean plasma rosuvastatin concentration–time profiles of each institution are shown in Figure 2 and the mean PK parameters determined by NCA are summarized in Table 2. The geometric mean ratios (GMRs) for treatment (rosuvastatin with telmisartan/rosuvastatin alone) observed in the three institutions were 2.3–2.9 for $C_{max,ss}$ and 1.3–1.4 for $AUC_{\tau,ss}$. GMRs of PK parameters ($C_{max,ss}$ and $AUC_{\tau,ss}$) between institutions (Inst_B/Inst_A or Inst_C/Inst_A) were 1.5–2.1 for $C_{max,ss}$ and 1.5–2.0 for $AUC_{\tau,ss}$. Median T_{max} value changed from 3–4 h for the rosuvastatin alone group to 1 h for the telmisartan coadministration group.

Table 2. Noncompartmental analysis results of rosuvastatin

Institution	Rosuvastatin alone (TRT1)				Rosuvastatin with Telmisartan (TRT2)				Ratio (TRT2 / TRT1)	
	$C_{max,ss}$ (ng/mL)	$AUC_{\tau,ss}$ (ng·h/mL)	$T_{max,ss}$ (h)	$t_{1/2}$ (h)	$C_{max,ss}$ (ng/mL)	$AUC_{\tau,ss}$ (ng·h/mL)	$AUC_{\tau,ss}$ (h)	$t_{1/2}$ (h)	$C_{max,ss}$	$AUC_{\tau,ss}$
A	23.3 (10.5)	194.6 (74.1)	4 (1-5)	7.5 (2.7)	55.3 (29.2)	260.1 (99.8)	1 (0.5-3)	10.4 (8.9)	2.3	1.4
B	41.4 (25.2)	381.4 (197.6)	3 (1-5)	9.9 (2.4)	116.5 (53.3)	522.0 (209.2)	1 (0.33-2)	11.3 (2.9)	2.9	1.4
C	36.1 (20.0)	302.1 (137.7)	4 (0.66-5)	8.8 (2.6)	88.5 (48.7)	385.0 (154.9)	1 (0.66-2)	12.6 (4.2)	2.4	1.3
Ratio (B/A)	1.6	1.8			2.1	2				
Ratio (C/A)	1.5	1.5			1.6	1.5				

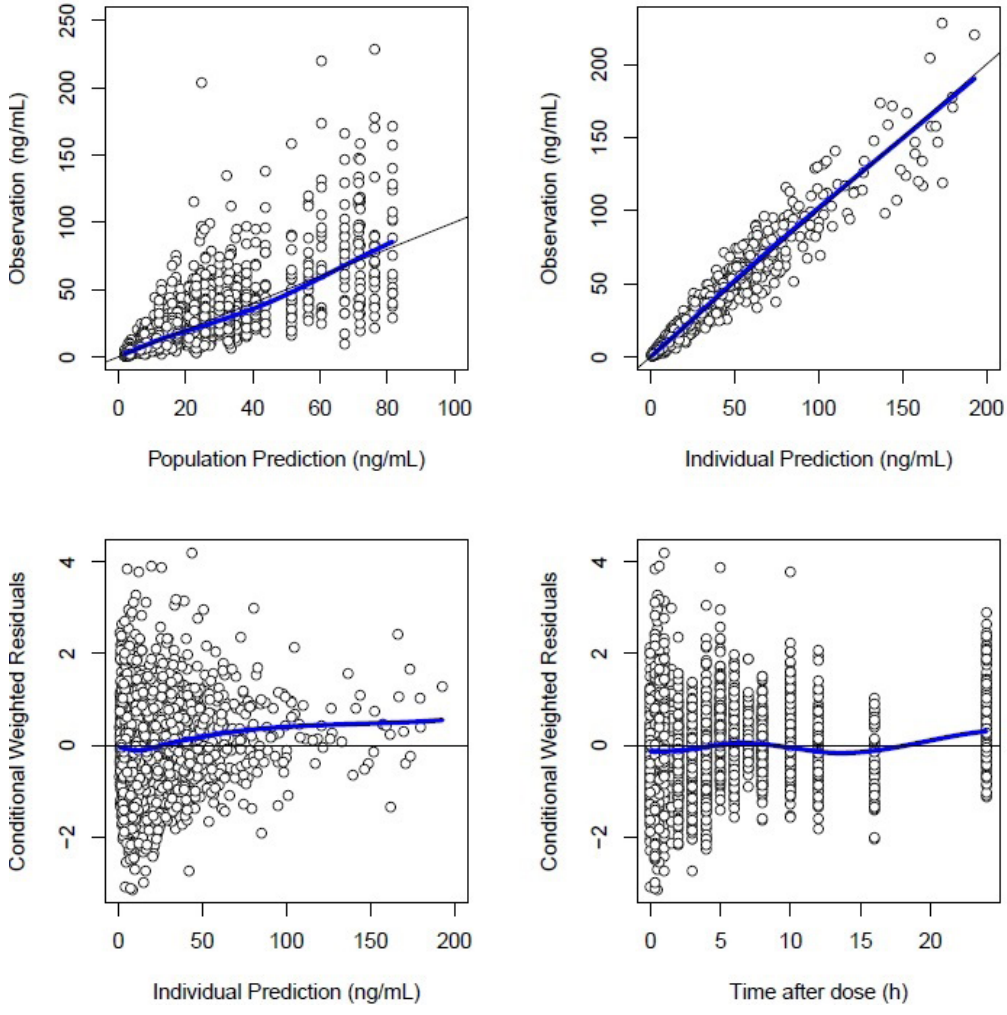

Figure 4. Basic goodness-of-fit plots of the final model. The grey solid y = x or y = 0 lines are included for reference. The bold blue lines are the loess (local regression smoother) trend lines.

Table 3. Summary of final population PK parameter estimates

Parameter	Description	Estimate	% RSE[a]	Bootstrap median (95% CI)[b]
Structural model				
CL/F (L/h)	Apparent clearance	106	11.5	103 (88.2-111)
Vc/F (L)	Apparent volume of central compartment	426	14.8	404 (339-449)
Q/F (L/h)	Apparent intercompartmental clearance	48.2	13.0	47.8 (38.8-54.8)
Vp/F (L)	Apparent volume of peripheral compartment	829	16.6	778 (634-969)
Without Telmisartan				
K_{a1} (h^{-1})	Absorption rate constant of Erlang absorption without telmisartan	0.910	11.8	0.912 (0.815-0.974)
Fr1	Fraction absorbed by Erlang absorption	0.197	20.7	0.200 (0.160-0.238)
D2 (h)	Duration of dosing for zero-order absorption	3.56	4.8	3.56 (3.41-3.75)
With Telmisartan				
K_{a2} (h^{-1})	Absorption rate constant of Erlang absorption with telmisartan	9.77	8.0	9.82 (8.61-11.2)
F_{rel}	Relative bioavailability of rosuvastatin with telmisartan when that without telmisartan assumed to be 1	1.30	4.3	1.29 (1.23-1.37)
Inter-study difference (INST)				
Inst_A	Fixed study difference of Inst_A	1.0 (Fixed)	-	-
Inst_B	Fixed study difference of Inst_B compared to Inst_A	1.58	9.1	1.54 (1.19-1.96)
Inst_C	Fixed study difference of Inst_C compared to Inst_A	1.48	9.6	1.44 (1.15-1.87)
Inter-individual variability				
$\omega_{CL/F}$ (%)	Interindividual variability of CL/F	43.3	13.1	40.9 (34.6-46.7)
$\omega_{Vc/F}$ (%)	Interindividual variability of Vc/F	64.8	11.7	58.7 (49.3-66.3)
$\omega_{Vp/F}$ (%)	Interindividual variability of Vp/F	67.1	16.0	61.1 (49.0-73.3)
$\omega_{Q/F}$ (%)	Interindividual variability of Q/F	60.6	11.9	54.0 (41.7-68.3)
ω_{ka1} (%)	Interindividual variability of K_{a1}	19.7	38.6	19.8 (0.40-40.6)
ω_{ka2} (%)	Interindividual variability of K_{a2}	49.0	14.5	45.8 (37.7-53.9)
ω_{Frel} (%)	Interindividual variability of F_{rel}	22.0	13.1	21.7 (16.7-25.0)
$\rho_{CL/F\sim Vc/F}$	Correlation coefficient between CL/F and V_c/F	0.920	12.9	0.919 (0.874-0.952)
$\rho_{CL/F\sim Vp/F}$	Correlation coefficient between CL/F and V_p/F	0.941	14.2	0.945 (0.880-0.999)
$\rho_{Vc/F\sim Vp/F}$	Correlation coefficient between Vc/F and V_p/F	0.971	12.7	0.973 (0.900-1.000)
Residual error				
σ_{add} (ng/mL)	Additive error	0.292	19.6	0.289 (0.103-0.406)
σ_{prop}	Proportional error	0.202	1.8	0.201 (0.190-0.217)

[a]Relative standard error, [b]95% confidence interval (CI) was estimated by applying the final population PK model to 200 re-sampled datasets.

Population PK Model Development

Exploratory analysis and the NCA results indicated that the plasma concentration–time profiles and the change of systemic exposures were similar among the institutions, thus model development started with a subset (Inst_A and rosuvastatin only group). Because the first-order absorption model showed a clear trend at early time points in the conditional weighted residual (CWRES) versus time plot, different absorption models were explored: the simultaneous first-order and zero-order absorption model clearly improved the goodness-of-fit. However, Er-

TCP
Transl Clin Pharmacol

lang absorption combined with a zero-order absorption model was best because many participants showed delayed absorption profiles. Thus, a two-compartment, first-order elimination model with simultaneous Erlang (fraction: Fr1) and zero-order (fraction: Fr2=1-Fr1) absorption described the PK profiles of rosuvastatin (without telmisartan) better than any other model (Fig. 3). After base model development with the subset, "rosuvastatin alone" PK data from all of the three institutions (Inst_A, Inst_B, and Inst_C) were analyzed simultaneously. Based on the difference of systemic exposure between institutions in NCA result (Table 2), the relative bioavailability (BA) between institutions was estimated by assuming the BA of the Inst_A equals 1

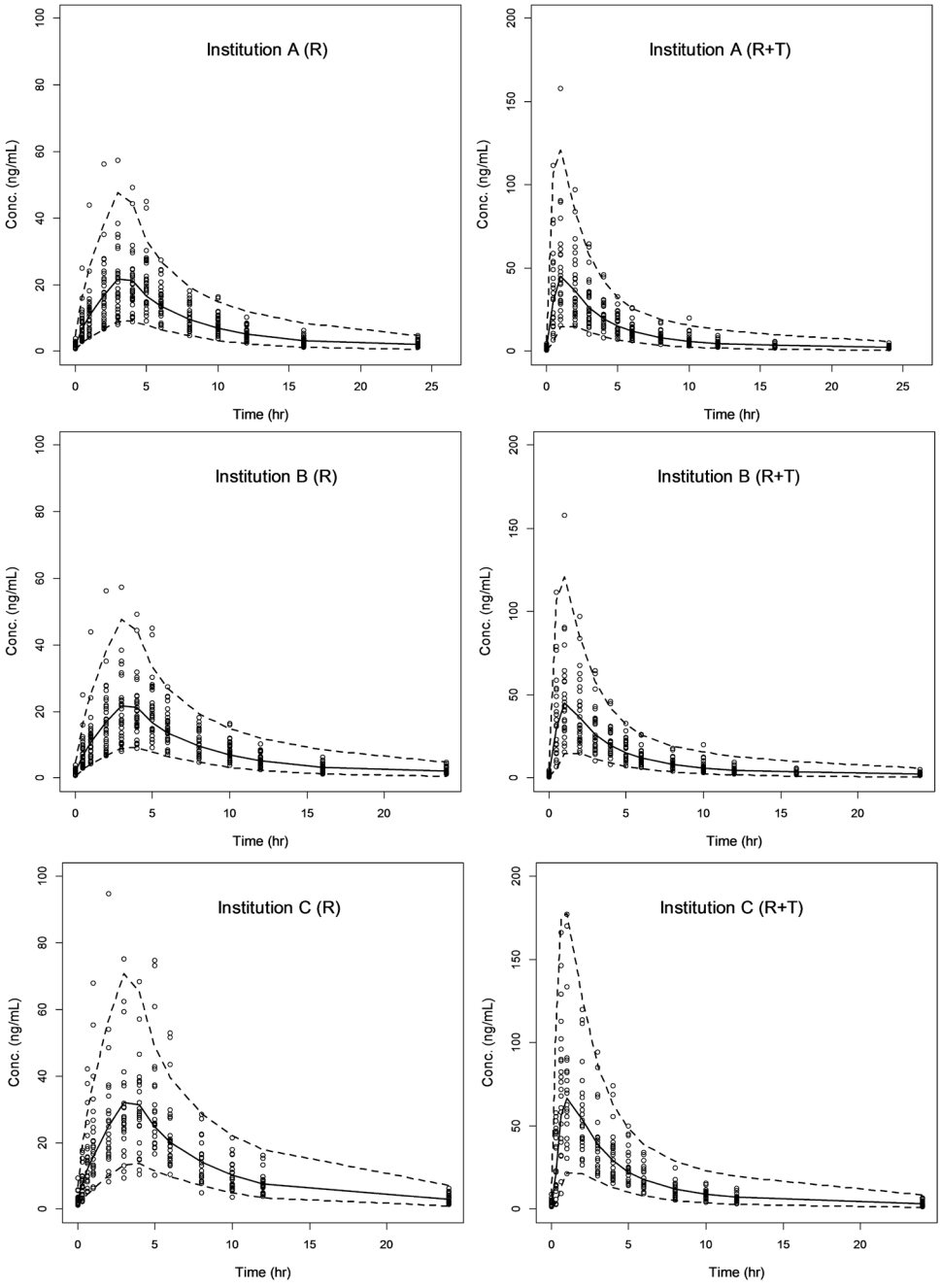

Figure 5. Visual predictive check for the final model by each institution (Institution A, B and C) and treatment group (R; rosuvastatin alone, R+T; rosuvastatin with telmisartan). The circles show the observed rosuvastatin concentrations. The solid and dashed lines show median and 90% prediction intervals of simulation, respectively.

as in the following equations:

$$Fr1 = P_{Fr1} \cdot P_{INST}$$
$$Fr2 = (1 - P_{Fr1}) \cdot P_{INST}$$

where P_{Fr1} is the fraction of Erlang absorption and P_{INST} is the ratio of Inst_B or C compared to Inst_A (The P_{INST} of Inst_A was fixed to 1).

When telmisartan was coadministered, the absorption of rosuvastatin was too fast to estimate both of the Erlang and zero-order absorption fractions: thus, the Erlang absorption model without a zero-order absorption term was chosen. Another relative bioavailability parameter for telmisartan treatment (F_{rel}) was also estimated to reflect the *AUC* changes by telmisartan. Because GMRs of $AUC_{\tau,ss}$ (with/without telmisartan) were similar among the institutions in the NCA results (Table 2), the interinstitutional difference of F_{rel} was not estimated. However, telmisartan treatment did not have an impact on CL/F (data not shown). Interindividual variability of CL/F, V_c/F, Q/F, V_p/F, k_{a1}, k_{a2}, and F_{rel} with a covariance structure (3 × 3 matrix of CL/F, V_c/F, and V_p/F) was incorporated into the structural model. The residual error was estimated using the combined additive and proportional error model. Goodness-of-fit plots suggest that the final model adequately described the observed concentration data (Fig. 4). The final parameter estimates are summarized in Table 3.

Median values of the parameter estimates and their 95% CIs from bootstrapping were very similar to the mean population estimates from the final model (Table 3). VPC results for both treatments (rosuvastatin with/without telmisartan) are shown in Figure 5.

Discussion

This analysis aimed to develop the population PK model of rosuvastatin using data from three PK drug interaction studies to evaluate the effect of telmisartan on rosuvastatin in Korean healthy volunteers. A two-compartment, first-order elimination with a simultaneous Erlang and zero-order absorption model was found best to fit the rosuvastatin data alone, which was consistent with a previously reported PK model except that a Erlang absorption component was used instead of first-order absorption.[13] The fraction and duration of zero-order absorption were 80.3% and 3.56 h, respectively, consistent with a previous report (86% and 4.48 h).[13] Two separate absorption rate constants (K_{a1} and K_{a2}) were also used to fit the altered absorption profile in telmisartan coadministration group.

There are mechanistic approaches such as physiologically based PK (PBPK) modeling using specialized software (Simcyp, Gatroplus, and PKsim)[14-16] and reduced (or simplified) PBPK modeling using NONMEM.[17,18] Rosuvastatin is a substrate of hepatic uptake transporters (OATP1B1, OATP1B3, OATP2B1, and NTCP) and efflux transporters such as BCRP, and there are many clinically meaningful DDI data.[15,19,20] Telmisartan is an inhibitor of MRP, BCRP in *in vitro*,[21] but, as yet, there is no reported case of clinical transporter-mediated DDI of telmisartan as a perpetrator. In our final model, telmisartan affects the absorption process of rosuvastatin rather than its metabolic elimination. Our model may be used as a starting point of mechanistic modeling to investigate the mechanism of rosuvastatin–telmisartan DDI.

In this study, we assumed that the difference of the mean PK exposure parameters (C_{max}, AUC_{τ}) among the institutions comes from the assay accuracy difference among the drug concentration assays (all of the three institutions used different CROs to assay rosuvastatin concentration). Laporte-Simitsidis et al.[22] showed that omitting the interstudy variability (ISV) does not introduce any bias into the estimation of the fixed effects or the residual variance terms, but does inflate the estimate of IIV. They recommended that it is probably not worth estimating ISV when the number of studies being pooled is less than 20. ISV estimated as relative BA in our model were 1.58 and 1.48 when that of Inst_A was fixed to 1. Although its implication may not be concluded in this report, we find it meaningful that the magnitude of ISV for PK assay in clinical trials, which has been discussed rarely in Korea, is reported herein.

In conclusion, the population PK model adequately described rosuvastatin and telmisartan DDI data. Increased exposure of rosuvastatin by telmisartan coadministration was mainly caused by the accelerated absorption rather than decreased clearance.

Conflict of interest

The authors declared no conflict of interest.

References

1. Rubba P, Marotta G, Gentile M. Efficacy and safety of rosuvastatin in the management of dyslipidemia. Vasc Health Risk Manag 2009;5:343-352.
2. Martin PD, Warwick MJ, Dane AL, Brindley C, Short T. Absolute oral bioavailability of rosuvastatin in healthy white adult male volunteers. Clin Ther 2003;25:2553-2563.
3. Martin PD, Mitchell PD, Schneck DW. Pharmacodynamic effects and pharmacokinetics of a new HMG-CoA reductase inhibitor, rosuvastatin, after morning or evening administration in healthy volunteers. Br J Clin Pharmacol 2002;54:472-477.
4. White CM. A review of the pharmacologic and pharmacokinetic aspects of rosuvastatin. J Clin Pharmacol 2002;42:963-970.
5. Bergman E, Forsell P, Tevell A, Persson EM, Hedeland M, Bondesson U, et al. Biliary secretion of rosuvastatin and bile acids in humans during the absorption phase. Eur J Pharm Sci 2006;29:205-214.
6. Kitamura S, Maeda K, Wang Y, Sugiyama Y. Involvement of multiple transporters in the hepatobiliary transport of rosuvastatin. Drug Metab Dispos 2008;36:2014-2023.
7. Ho RH, Tirona RG, Leake BF, Glaeser H, Lee W, Lemke CJ, et al. Drug and bile acid transporters in rosuvastatin hepatic uptake: function, expression, and pharmacogenetics. Gastroenterology 2006;130:1793-1806.
8. Lee E, Ryan S, Birmingham B, Zalikowski J, March R, Ambrose H, et al. Rosuvastatin pharmacokinetics and pharmacogenetics in white and Asian subjects residing in the same environment. Clin Pharmacol Ther 2005;78:330-341.
9. Jamei M, Bajot F, Neuhoff S, Barter Z, Yang J, Rostami-Hodjegan A, et al. A mechanistic framework for in vitro-in vivo extrapolation of liver membrane transporters: Prediction of drug-drug interaction between rosuvas-

tatin and cyclosporine. Clin Pharmacokinet 2014;53:73-87. doi: 10.1007/s40262-013-0097-y.

10. Hua WJ, Hua WX, Fang HJ. The role of OATP1B1 and BCRP in pharmacokinetics and DDI of novel statins. Cardiovasc Ther 2012;30:e234-e241. doi: 10.1111/j.1755-5922.2011.00290.x.
11. Johnson ML, Pietz K, Battleman DS, Beyth RJ. Prevalence of comorbid hypertension and dyslipidemia and associated cardiovascular disease. Am J Manag Care 2004;10:926-932.
12. Son M, Kim Y, Lee D, Roh H, Son H, Guk J, et al. Pharmacokinetic interaction between rosuvastatin and telmisartan in healthy Korean male volunteers: a randomized, open-label, two period, crossover, multiple-dose study. Clin Ther 2014;36:1147-1158.
13. Tzeng TB, Schneck DW, Birmingham BK, Mitchell PD, Zhang H, Martin PD, et al. Population pharmacokinetics of rosuvastatin: implications of renal impairment, race, and dyslipidaemia. Curr Med Res Opin 2008;24:2575-2585. doi: 10.1185/03007990802312807.
14. Bolger MB, Lukacova V, Woltosz WS. Simulations of the nonlinear dose dependence for substrates of influx and efflux transporters in the human intestine. AAPS J 2009;11:353-363.
15. Jamei M, Bajot F, Neuhoff S, Barter Z, Yang J, Rostami-Hodjegan a, et al. A mechanistic framework for in vitro-in vivo extrapolation of liver membrane transporters: Prediction of drug-drug interaction between rosuvastatin and cyclosporine. Clin Pharmacokinet 2014;53:73-87. doi: 10.1007/s40262-013-0097-y.
16. Jones HM, Mayawala K, Poulin P. Dose selection based on physiologically based pharmacokinetic (PBPK) approaches. AAPS J 2013;15:377-387.
17. Gertz M, Tsamandouras N, Säll C, Houston JB, Galetin A. Reduced 233 Physiologically-Based Pharmacokinetic Model of Repaglinide: Impact of OATP1B1 and CYP2C8 Genotype and Source of In Vitro Data on the Prediction of Drug-Drug Interaction Risk. Pharm Res 2014;31:2367-2382.
18. Tsamandouras N, Dickinson G, Guo Y, Hall S, Rostami-Hodjegan A, Galetin A, et al. Development and Application of a Mechanistic Pharmacokinetic Model for Simvastatin and its Active Metabolite Simvastatin Acid Using an Integrated Population PBPK Approach. Pharm Res 2015;32:1864-1883.
19. Schneck DW, Birmingham BK, Zalikowski JA, Mitchell PD, Wang Y, Martin PD, et al. The effect of gemfibrozil on the pharmacokinetics of rosuvastatin. Clin Pharmacol Ther 2004;75:455-463.
20. Chauvin B, Drouot S, Barrail-Tran A, Taburet AM. Drug-drug interactions between HMG-CoA reductase inhibitors (statins) and antiviral protease inhibitors. Clin Pharmacokinet 2013;52:815-831.
21. Weiss J, Sauer A, Divac N, Herzog M, Schwedhelm E, Böger RH, et al. Interaction of angiotensin receptor type 1 blockers with ATP-binding cassette transporters. Biopharm Drug Dispos 2010;31:150-161.
22. Laporte-Simitsidis S, Girard P, Mismetti P, Chabaud S, Decousus H, Boissel JP. Inter-study variability in population pharmacokinetic meta-analysis: When and how to estimate it? J Pharm Sci 2000;89:155-167.